Journal of Materials Chemistry A

RSC Publishing

PAPER

View Article Online
View Journal | View Issue



# Covalently bonded interfaces for polymer/graphene composites†

Cite this: *J. Mater. Chem. A*, 2013, **1**, 4255

Jun Ma,[ab] Qingshi Meng,[b] Andrew Michelmore,[c] Nobuyuki Kawashima,[c] Zaman Izzuddin,[b] Carl Bengtsson[b] and Hsu-Chiang Kuan*[ab]

Received 28th November 2012
Accepted 18th January 2013

DOI: 10.1039/c3ta01277h

www.rsc.org/MaterialsA

The interface is well known for taking a critical role in the determination of the functional and mechanical properties of polymer composites. Previous interface research has focused on utilising reduced graphene oxide that is limited by a low structural integrity, which means a high fraction is needed to produce electrically conductive composites. By using 4,4′-diaminophenylsulfone, we in this study chemically modified high-structural integrity graphene platelets (GnPs) of 2–4 nm in thickness, covalently bonded GnPs with an epoxy matrix, and investigated the morphology and functional and mechanical performance of these composites. This covalently bonded interface prevented GnPs stacking in the matrix. In comparison with unmodified composites showing no reduction in electrical volume resistivity, the interface-modified composite at 0.489 vol% GnPs demonstrates an eight-order reduction in the resistivity, a 47.7% further improvement in modulus and 84.6% in fracture energy release rate. Comparison of GnPs with clay and multi-walled carbon nanotubes shows that our GnPs are more advantageous in terms of performance and cost. This study provides a novel method for developing interface-tuned polymer/graphene composites.

## 1 Introduction

Graphene, a single layer of graphite, is a monolayer of $sp^2$ hybridized carbon atoms arranged in a hexagonal lattice. Properties such as high electron conductivity, the quantum hall effect at ambient temperatures, impeccable strength and controllable band gaps are of particular interest in this material.[1–3] Pristine graphene cannot be used as a filler for polymer composites due to its high manufacturing cost, inappropriate lateral size and lack of functional groups[4,5] for bonding with polymers. Thus, preceding studies adopted graphene oxide (GnO) which was fabricated by heavy oxidation and contains rich functional groups for interface modification of polymer composites. Various chemical and thermal reduction methods have endeavored to restore the integrity, but unfortunately these methods cannot restore most of the integrity. For example, the $I_D/I_G$ ratio from Raman spectra of thermally reduced graphene oxide was seen to be higher than 1.0 in comparison to graphene platelets (GnPs) being a minor 0.06.[6,7] We herein tentatively defined GnPs as a graphene derivative where each platelet should be less than 10 nm in thickness, since the specific surface area of platelets in a composite markedly reduces when the platelets are thinner than 10 nm. Since up to ~1 nm-thick, single-layer graphene was fabricated by previous studies using thermal expansion,[8,9] these GnPs should contain no more than 10 layers of graphene. Advantages of GnPs include: (i) high structural integrity, (ii) the presence of epoxide groups which can react with the end-amine groups of organic molecules to form stable colloids and to build up a robust interface with the matrix, (iii) low fabrication cost at 10–20 US$ per kg, and (iv) low thickness for maximum resemblance of its sister graphene's properties.

Of all the engineering materials, polymers have seen the most rapid increase in industrial applications, but they have limitations. Some polymers such as epoxy resins are inherently brittle in nature and are limited in their application; conducting polymers need to further improve their conductivity and robustness for energy storage applications. Through the process of combining polymers with nano-additives to produce nanocomposites, it has been proven that with homogenous dispersion, these limitations can be alleviated or removed.[10,11] Clay features a layered structure, which, when mixed with epoxies, has been confirmed to improve their toughness. Their limitation lies in their conductivity and compatibility with polymers.[7] A nanocomposite possesses an exceptional interface area to filler volume, and as a result exhibits significant load/electron/phonon transfer across the interface.

An interface can be described as the linking region between the matrix and dispersion phase, and theoretically it is the link that bonds the constituting entities. The role of the interface

[a]Department of Energy Application Engineering, Far East University, Tainan City 744, Taiwan. E-mail: hckuan@cc.feu.edu.tw; Tel: +886-922948363

[b]School of Engineering, University of South Australia, SA5095, Australia

[c]Mawson Institute, University of South Australia, SA5095, Australia

† Electronic supplementary information (ESI) available. See DOI: 10.1039/c3ta01277h

has a central part in the overall mechanical and functional performance of polymer nanocomposites and as a result a great deal of effort is being placed into the interface bonding.[12–14] As part of the nanocomposite structure, the interface can either be the yielding point or strong point relative to the properties of those materials it is bonded with. The latter means that an interface transfers loading from matrix to dispersion phase, carries over electrons and phonons, and transports thermal energy efficiently. An exceptional interface region from inorganic to organic can be as long as a few centimeters,[15] but it is often difficult to measure an interface thickness in polymer nanocomposites.

A hypothesis made herein was that, upon interface modification, graphene platelets (GnPs) should show a more uniform dispersion and a higher degree of stress and electron transfer across the interface, leading to more increments in fracture toughness and electrical conductivity. On the other hand, it may pose a barrier to electrical conductivity, causing a higher percolation threshold of electron mobility.

We will in this study design and fabricate a covalently bonded interface for epoxy/graphene nanocomposites, investigate their functional, mechanical and thermal dynamic properties, and identify the structure–property relations of these composites.

## 2 Experimental

### 2.1 Materials

A graphite intercalation compound (GIC, Asbury 3494) was provided by Asbury Carbons, Asbury, NJ, USA. Tetrahydrofuran (THF), 1-methy-2-pyrrolidone 99% (NMP), 4,4′-diaminodiphenylsulfone (DDS) and triisopropanolamine (TIPA) were purchased from Sigma Aldrich. Polyoxyalkyleneamine (Jeffamine D230, $M_w$ 230), provided by Huntsman, was used as a hardener due to its popularity and commercial availability. Epoxy resin, diglycidyl ether of bisphenol A (DGEBA, Araldite-F) with epoxide equivalent weight 182–196 g per equiv., was purchased from Ciba-Geigy, Australia. Fig. 1 contains the molecular formulae of DDS and DGEBA.

### 2.2 Modification of graphene platelets

Graphene platelets (GnPs) were fabricated according to a reported procedure.[7] In brief, 0.5 g GIC was heated at 700 °C in a furnace for 1 min to produce expanded graphite; the expanded product was suspended in acetone and upon ultrasonication, produced GnPs. A calculated amount of GnPs was suspended in NMP (0.1 wt%) in a metal container, followed by sonication for 30 min at a temperature below 30 °C. Calculated amounts of TIPA as a catalyst and DDS as a modifier were added to the mixture while stirring to dissolve fully, followed by another sonication at a temperature below 30 °C for 1 h. The mixture was then transferred into a round-bottom flask with a condenser and kept reacting at 150 °C for 32 h, to produce DDS-modified GnPs. The weight ratio of TIPA/DDS/GnPs was controlled at 8.28/5.00/0.10. The mixture was then washed by acetone at least three times to remove the excess DDS. The final process of graphene modification proceeded through the suspension of a calculated amount of DDS-modified GnPs in NMP (0.1 wt%) using a metal container followed by sonication for 30 min at a temperature below 30 °C. DGEBA was then added to the mixture, followed by another sonication for 30 min below 30 °C. After sonication, the mixture was transferred into a round-bottom flask with a condenser and kept reacting at 150 °C for 4 h. Finally, the sample was washed again using acetone at least three times to remove excess DGEBA that was not used in the grafting stage. This produced further modified GnPs (m-GnPs). Fig. S1† shows a schematic mechanism of the graphene modification.

### 2.3 Fabrication of epoxy/m-GnP nanocomposites

A weighed quantity of m-GnPs was suspended at 0.1 wt% in THF using a metal container followed by stirring for 10 min using a magnetic bar. The container was then covered and treated in an ultrasonic bath for 30 min below 30 °C to obtain a homogenous suspension of the platelets. DGEBA was added to the mixture and then stirred using a magnetic bar for 10 min at room temperature to dissolve completely, followed by sonication under 30 °C for 1 h. The temperature was proved to be significantly important in aiding the exfoliation and dispersion of graphite layers, as noted by Ma *et al.*[16] After sonication the solvent (THF) was evaporated at 120 °C using a mechanical mixer without a condenser, followed by vacuum oven-degassing at 120 °C to remove bubbles. The mixture was then cooled down to ~40 °C, followed by addition of hardener (J230) and mixing for two minutes. The mixture was degassed at room temperature and poured into preheated and greased rubber

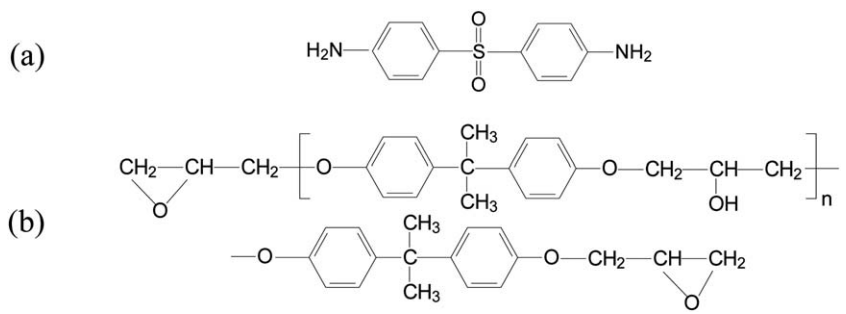


**Fig. 1** Molecular formula of (a) 4,4′-diaminodiphenylsulfone (DDS) and (b) diglycidyl ether of bisphenol A (DGEBA).

 

moulds and cured using an appropriate procedure. Curing employed the following procedure: (i) a temperature of 80 °C was set to be achieved within 30 min, (ii) maintained for 150 min, (iii) the temperature was then raised to 120 °C within 30 min, (iv) maintained for 12 h, and (v) for the final stage the specimens were left in the oven until the oven had become cool.

### 2.4 Characterization

**2.4.1 Filler modification.** A Perkin Elmer 65 FT-IR spectrometer with a Miracle Single Reflection ATR Sample Accessory was used to examine samples within the range of 4000–450 $cm^{-1}$ at 2 $cm^{-1}$ for a minimum of 32 scans. Raman spectra were recorded on a Renishaw inVia Raman micro-spectrometer with 633 nm laser excitation.

X-ray diffraction (XRD) was performed using a diffraction technology mini-materials analyser on the graphite intercalation compound, GnPs, and m-GnPs and their nanocomposites. The diffractometer was equipped with curved graphite monochromators, tuned to Cu K$\alpha$ radiation ($\lambda$: 1.5419 Å) with tube voltage applied at 35 kV and 28.2 mA (1 kW). The diffraction patterns were collected in a reflection mode geometry between $2\theta$ = 2–50° at 1° $min^{-1}$. High-resolution XPS measurements were carried out using a SPECS SAGE XPS system with a Phoibos 150 analyser and an MCD-9 detector, which used non-monochromated Mg K$\alpha$ radiation at 10 kV and 20 mA (200 W).

AFM images were taken of the GnPs with a NT-MDT SPM instrument with NSG03 non-contact "golden" cantilevers. The samples were prepared by suspending GnPs in *N*-methyl-2-pyrrolidone (NMP) at 0.0004 wt% by 30 min ultrasonication and then dropping the solution on a silicon wafer followed by drying. The roughness of the silicon wafer was measured independently to be <0.2 nm.

A Leica Ultracut S microtome and a diamond knife were used at room temperature to produce 50 nm-thin sections. Sections were collected through 200-mesh copper grids, and then examined *via* a Philips CM200 transmission electron microscope (TEM) at 200 kV.

**2.4.2 Functionality, mechanical performance and fracture toughness of nanocomposites.** The volume resistivity of the samples of 6.8 ± 2.1 mm in thickness and 24 ± 0.2 mm in diameter was measured at room temperature with an Agilent 4339B high resistivity meter equipped with a 16008B resistivity cell. The samples were tightly screw-pressed between two cylindrical electrodes which have a diameter of 26 mm. In order to provide stable values of resistivity, the sample surface was finely polished to ensure good electrical contact.

Tensile dumb-bell samples were produced with the use of silicone rubber molds. Prior to testing, both sides of the samples specimens were polished using emery paper to remove all visible marks and imperfections. Tensile testing was conducted through the use of an Instron 5567 tensile machine at the speed of 0.5 mm $min^{-1}$ and at room temperature. An Instron extensometer 2630-100 was used to collect accurate displacement data for the modulus measurement which was calculated using 0.005–0.2% strain.

Fracture toughness was measured by compact tension (CT) samples. An instantly propagated crack was introduced to each sample through the razor blade tapping method,[17,18] and at least four specimens at a speed of 0.5 mm $min^{-1}$ were tested for each set of data. The values of $K_{1c}$ and $G_{1c}$ were calculated and then verified according to ISO13586.

The density of graphene was taken as that of graphite 2.26 g $cm^{-3}$; the density of matrix was assumed to be 1.1 g $cm^{-3}$. Thus, we were able to convert wt% to vol%.

## 3 Results and discussion

### 3.1 Interface build up

Pristine graphene cannot be used to compound with epoxy due to a lack of reactive sites for interface modification of nanocomposites. Thus, reduced graphene oxide has been extensively studied in spite of its low structural integrity and added cost due to the reduction. In this study, we thermally expanded a commercial graphite intercalation compound at 700 °C for 1 min and treated the expanded product with ultrasonication to produce graphene platelets (GnPs). When dispersed in *N*-methyl-2-pyrrolidone (NMP), the GnP thickness was measured as 2.51 ± 0.39 nm.[5] Epoxide groups of GnPs are found by XPS analysis in Fig. 2, in agreement with previous studies where similar groups were reported in thermally treated graphene oxide.[19,20] To build up a strong interface for epoxy/graphene nanocomposites, diaminodiphenylsulfone (DDS) was chosen to react with the epoxide groups of the GnPs. It is worth mentioning that the epoxide groups of GnPs are not sufficiently active to react with the hardener J230 to produce crosslinking; and they also lack in quantity. DGEBA's epoxides take the form of an equilateral triangle which causes a straining of the atoms. The straining causes the epoxides to exhibit a high reactivity for reaction with J230. Thus, a catalyst triisopropanolamine was adopted to provide an intense alkaline environment for this modification.

The quantity of DDS tripled the stoichiometric requirement, in order to reduce the chance of DDS bridging adjacent layers to produce thicker platelets. The ideal effect would be only one

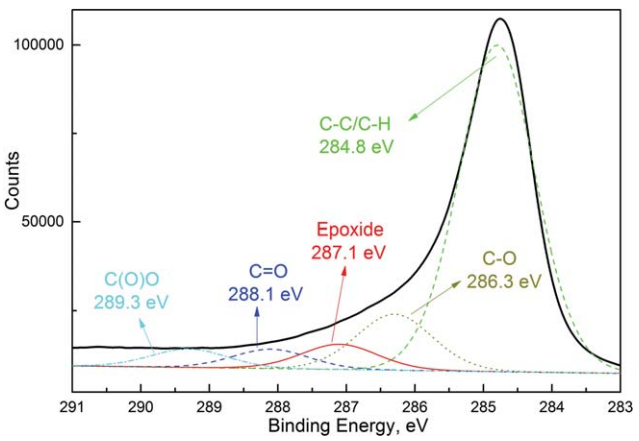


**Fig. 2** XPS analysis of the graphene platelets.

end-amine group of every DDS molecule grafting to GnPs. These DDS-modified GnPs were further reacted with theoretically only one end-epoxide group of a diglycidyl ether of bisphenol A (DGEBA) molecule.

Fig. 3 contains a schematic of the raw material – a graphite intercalation compound, where chemicals intercalate between graphene layers; the layer number between the intercalated chemicals is called a stage. A stage, generally ranging from 1 to 5, is actually a graphene platelet. The subsequent ultrasonication further separates and delaminates these GnPs. It is worth pointing out that the layered structure in each GnP should be retained through the modification and subsequent compounding with polymers. However, GnPs should be able to expand or even exfoliate themselves with a proper surface modification and compounding process.

We have verified the reaction between the GnPs' epoxide groups and DDS's end-amine groups with specific reaction times on the grafting efficiency. Upon reaction, new absorptions would be expected on the DDS-grafted GnPs. Fig. 4 contains the FTIR spectra of unmodified GnPs and these modified GnPs with different time slots, where four obvious new absorptions are seen for the modified GnPs: (i) two medium-intensity absorptions at 1604 and 1670 $cm^{-1}$ are due to complex molecular motions of the entire rings of DDS; (ii) one weak absorption at 2913 $cm^{-1}$ corresponds to C–H stretching; and (iii) a broad and intense absorption in the 3100 to 3400 $cm^{-1}$ range would be caused by the end-amine groups of DDS.[21] These provide a solid evidence for the grafting between the GnPs' epoxide groups and DDS's end-amine groups. To determine which reaction time is ideal in producing the highest grafting density, we employed software to calculate the area under the absorption at 1604 $cm^{-1}$ in Fig. 4. In Table 1, the absorption at 32 hours witnessed the highest intensity, and hence a mixing time of 32 hours was chosen to produce DDS-modified GnPs.

After a thorough washing process, DDS-modified GnPs were mixed and reacted with a superfluous amount of DGEBA (monomer of epoxy), which was thoroughly washed again to remove non-reacted DGEBA molecules; In this process the end-amine groups of DDS-modified GnPs would react with the epoxide groups of DGEBA, to produce m-GnPs. Fig. 5 contains spectra of the unmodified GnPs and m-GnPs. The following absorption evolution is observed for m-GnPs: (i) two absorptions at 2920 and 2848 $cm^{-1}$ correspond to C–H and $CH_2$–O bonds, (ii) one at 1660 $cm^{-1}$ disappeared, implying the reaction of the grafted end-amine groups with DGEBA, and (iii) one at 1509 $cm^{-1}$ may be caused by C–$H_3$ assymetric stretching or C–$H_2$ stretching.[22] All of this points towards the reaction of DGEBA with DDS-modified GnPs. This two-step modification

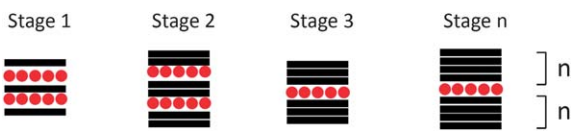


**Fig. 3** Schematic of the staging phenomenon in graphite intercalation compounds.

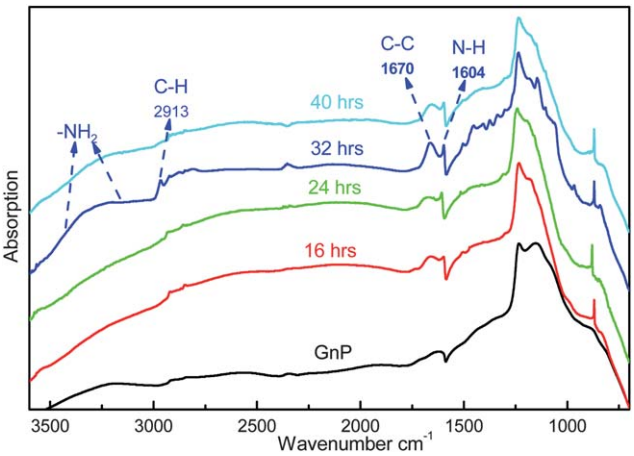


**Fig. 4** FTIR spectra of graphene platelets (GnPs) modified by diaminodiphenylsulfone (DDS).

can create a covalently bonded interface for epoxy/GnP nanocomposites, as schematically shown in Fig. 6.

Graphene features an exceptionally high in-plane electrical conductivity in comparison with orders of lower through-plane conductivity; while graphene is the stiffest and strongest material ever-measured, graphite consisting of graphene layers is a well-known lubricator. These phenomena demonstrate the importance of keeping GnPs as thin as possible. A low thickness produces the following benefits: (i) retaining the high mechanical strength of graphene, (ii) reducing the negative effect of through-plane conductivity, and (iii) yielding a high specific surface area, which implies more platelets in a given volume and fraction of composite. Since the bi-functional DDS and DGEBA used for the GnP surface modification may covalently link adjacent GnPs, we expected an increase in the GnP thickness. Thus we examined the thickness by AFM.

Fig. 7 contains a representative AFM micrograph and its height profile. Three types of GnPs are observed. (i) Thick platelets, as shown by an exceptionally large white platelet in the left figure, and its thickness was measured as ~20 nm; these platelets are rare; (ii) platelets of ~10 nm in thickness, as shown by a red arrow; and (iii) platelets of ~2.5 nm in thickness, as shown by a white arrow. Since the type (ii) and (iii) platelets are far more popular, over ten platelets of these types were randomly selected and their thickness was measured to be 6.4 ± 2.6 nm, as shown in Fig. S2.† Because surface modification started with GnPs of 2–4 nm in thickness,[7] the increase in platelet thickness after modification must be caused by the organic molecules used in the modification. Both DDS and DGEBA have bi-functional end groups, thus are capable of grafting two adjacent layers. These grafted adjacent layers cannot be separated any more in the following processes,

**Table 1** Effect of reaction time on the grafting efficiency of DDS

| Time, hour | 16 | 24 | 32 | 40 |
|---|---|---|---|---|
| Relative intensity at 1604 $cm^{-1}$ | 1.00 | 1.11 | 2.22 | 1.44 |

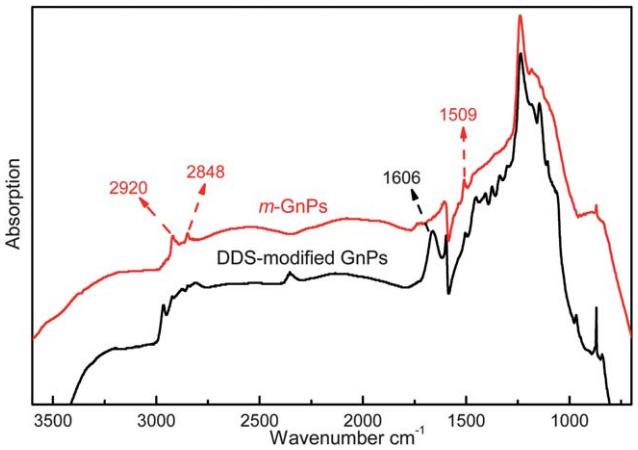


**Fig. 5** FTIR spectra of DDS-modified GnPs and m-GnPs.

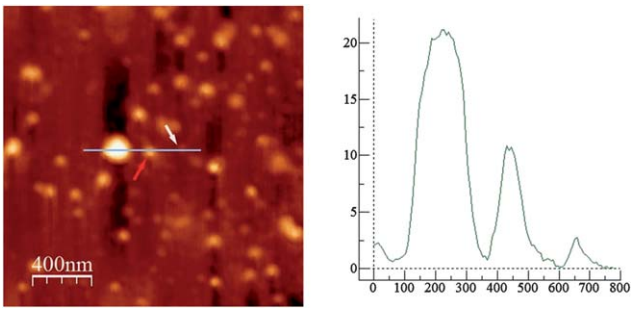


**Fig. 7** Characterization of graphene platelets using atomic force microscopy.

producing thicker GnPs. This implies that higher fractions of GnPs may be needed for the following fabrication of electrically conductive polymer composites. Since the composite electrical conductivity is mainly determined by its fillers' conductivity, we measured the structural integrity of GnPs by a Raman spectrometer – a high structural integrity of graphene always leads to an excellent electrical conductivity.

Both GnPs and m-GnPs show two absorptions at around 1350 and 1575 $cm^{-1}$ in Fig. 8. The D band refers to the absorption at 1350 $cm^{-1}$, and its intensity indicates the quantity of disordered structure, such as the voids caused by oxidation and reduction; the G band intensity at 1575 $cm^{-1}$ corresponds to the ordered structure of $sp^2$ hybridized carbon. Hence, the $I_D/I_G$ ratio indicates a degree of disorder. Practically, this ratio can be obtained by measuring the height or area of these two bands using Excel or other software; it is worth noting both the height and area are dependent on how the base line is chosen. Since the height ratio is more sensitive, it was adopted in this study. Fig. S3† shows the baselines selected in this study using Origin software. Both thermally and chemically reduced graphene oxide produced an $I_D/I_G$ ratio of ~1.0; by contrast, our GnPs demonstrate a significantly lower $I_D/I_G$ ratio of 0.07 in Fig. 8, aligning with our previous work.[5,7] The ratio decreases to 0.03 after the modification, because GnPs were heated in NMP at 150 °C for 36 h and this reduced GnPs. The comparison demonstrates the much higher structural integrity of m-GnPs. In previous graphene studies, dozens of hours of sonication produced a lot of defects in the product, leading to a reduction in the lateral size of graphene platelets and an increase in the $I_D/I_G$ ratio.[23,24] In comparison, the sonication time in this study is no longer than 2 h in total and thus its effect on the lateral dimension is trivial. It is worth to note that GnPs show D and G bands at 1359.2 and 1584.3 $cm^{-1}$, while these two bands shift to 1351.3 and 1581.7 $cm^{-1}$ for m-GnPs, respectively. These red shifts must be caused by the surface modification of GnPs. No obvious change is seen in the 2D absorption.

The 2-step surface modification of grafting organic molecules onto the GnPs, leads to an increase in the GnP thickness and their structural integrity. This may also produce some difference in the GnP layer spacing, which needs to be investigated by XRD.

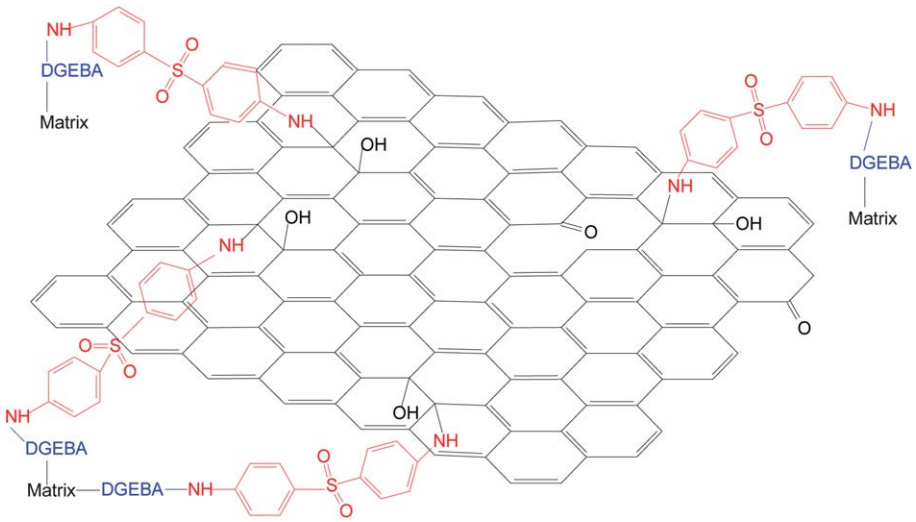


**Fig. 6** Atomic structures of the covalently bonded interface between the GnPs and matrix.

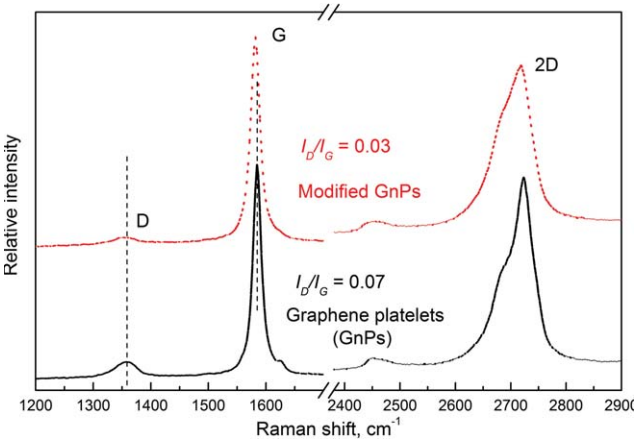


**Fig. 8** Raman spectra of graphene platelets (GnPs) and m-GnPs.

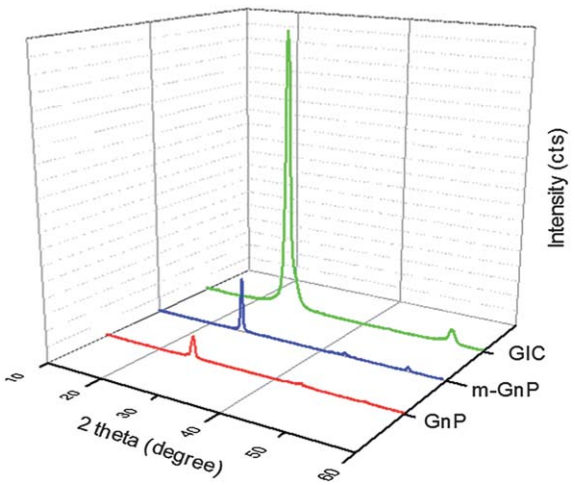


**Fig. 9** XRD patterns of the graphite intercalation compound (GIC), GnPs and m-GnP.

Fig. 9 shows XRD patterns of the graphite intercalation compound (GIC), graphene platelets (GnPs), modified GnPs (m-GnPs), all of which were thoroughly washed before characterization. GIC retaining the graphene-stacked structure exhibits a typical sharp and high intensity diffraction at 26.18°, indicating the presence of a large amount of a crystalline phase in the specimen with a distance of 0.34 nm interlayer spacing; this implies a high structural integrity of graphene, opposite to graphene oxide. GnPs demonstrate a diffraction pattern at the same angle, implying the retention of a graphene layer spacing of 0.34 nm. However, the intensity is largely reduced and this is explained in light of the GnP fabrication process. After thermal expansion and ultrasonication, GIC was converted into GnPs.[5,7] The thermal expansion and ultrasonication caused corrugation, voids, reduction in the lateral dimension, and increase in layer spacing between stages or even exfoliation, all of which contribute to the diffraction intensity reduction. The intensity of m-GnPs shows a slightly increased intensity, since the washing and modification procedures instigated a re-aligning and stacking of the wrinkled GnPs.

Since the diffraction angle does not change, we expected only a small fraction of organic molecules to be grafted with GnPs, which was identified by the following TGA analysis. Both GnPs and m-GnPs show an obvious mass loss from 100–200 °C, attributed to the deintercalation of $H_2O$. While GnPs demonstrate little further loss until 600 °C, an obvious loss is observed for m-GnPs, which must be caused by the grafted DDS and DGEBA. From room temperature to 600 °C, the loss values of GnPs and m-GnPs were 3.3 wt% and 9.5 wt%, respectively. The difference in these two values yields 6.2 wt% – the least weight fraction of the grafted molecules (Fig. 10).

### 3.2 Nanocomposites

As discussed in Fig. 3, graphene platelets (GnPs) may expand and exfoliate in solution or polymer matrices, while the layered graphene structure in each platelet should retain throughout the processing. Fig. 11a contains X-ray diffraction patterns of neat epoxy and epoxy/m-GnP nanocomposites. Neat epoxy shows a large diffraction from 11–27°, which is attributed to the scattering of cured epoxy molecules. While the 0.122 and 0.244 vol% nanocomposites show similar diffraction patterns to the neat epoxy's, the 0.489 vol% pattern indicates a tiny diffraction at $2\theta = 26.5°$, corresponding to an interlayer distance of 3.35 Å associated with the graphitic plane. Since the layered structure is maintained in each GnP, the nanocomposites should show more or less diffraction at ~26.5°. The significant diffraction of epoxy molecules must cover the GnP diffraction pattern at ~26.5° in the 0.122 and 0.244 vol% nanocomposites.

To illuminate the effect of this covalently bonded interface on the nanocomposites' structure, the diffraction pattern of the 0.244 vol% nanocomposite was compared in Fig. 11b with the same fraction nanocomposite reported in our previous work where epoxy was simply mixed with unmodified GnPs.[7] In the epoxy/unmodified GnP nanocomposite, we observe a sharp diffraction at 26° which is due to the stacked GnPs. However, this diffraction is invisible in the epoxy/m-GnPs nanocomposites, implying a lower degree of GnP stacking since the layered structure in each GnP should always be retained. The GnP surface modification by DDS and DGEBA builds up a

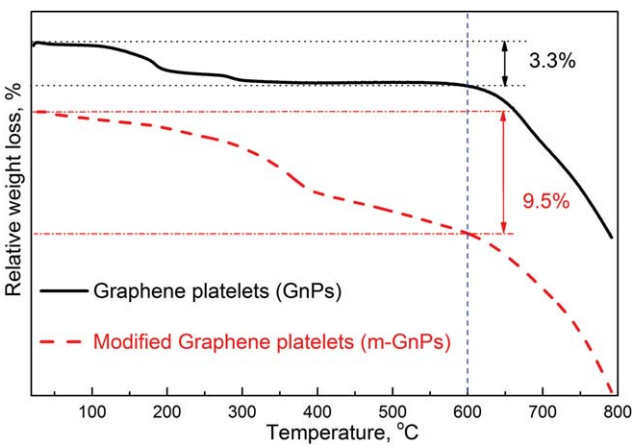


**Fig. 10** Weight loss of GnPs and m-GnPs in air.

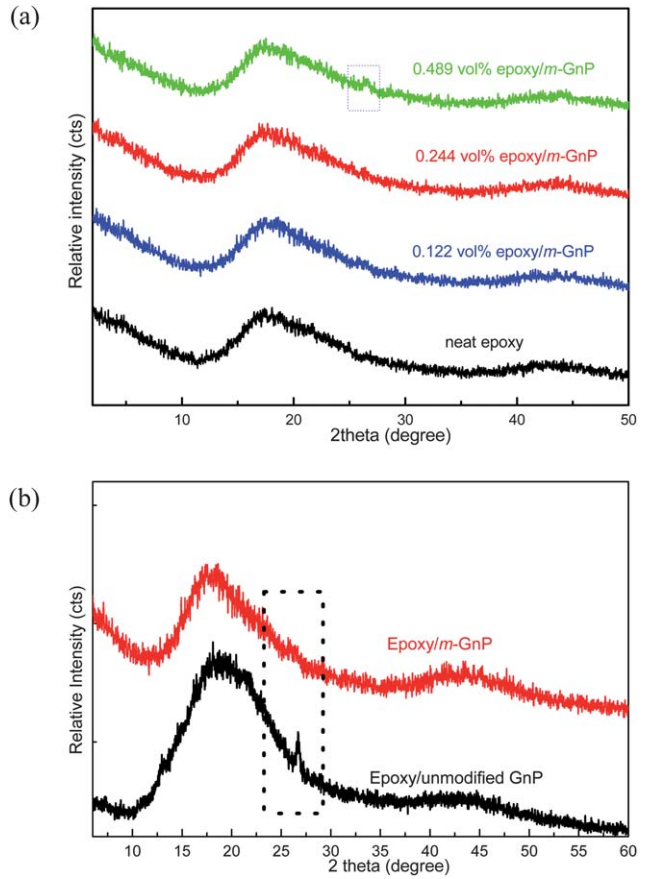


**Fig. 11** XRD patterns of (a) neat epoxy and its modified graphene platelet (m-GnP) nanocomposites and (b) comparison of epoxy/unmodified GnP nanocomposite with the modified one at 0.244 vol%.

covalently bonded interface, promoting the dispersion and delamination of GnPs in the matrix, and this explains the absence of the sharp 26° diffraction.

Transmission electron microscopy (TEM) was utilized to investigate the dispersion of GnPs in the matrix. In Fig. 12, the darker zones are due to the high crystallinity of GnPs relative to the amorphous cross-linked matrix which scattered fewer of the electrons during observation. Fig. 12a presents a low magnification micrograph of the 0.244 vol% nanocomposite, where voids, GnP clusters and separately dispersed GnPs are observed. Since graphene is the stiffest and strongest material that has ever been measured, there must be a high level of resistance in microtoming using a diamond knife, which produced the voids. The large stiffness contrast between GnPs and the matrix also contributes to the void formation. As discussed in AFM analysis, the reactive modifiers built up a covalent interface, which inevitably linked some adjacent GnPs, leading to a larger thickness. It also caused clusters. Nevertheless, separately dispersed GnPs are clearly observed, as pointed by white arrows. Representative voids and clusters were further investigated at higher magnifications in Fig. 12c. Features observed included (i) the formation of tube-like or fibre-like morphology, as shown by a white arrow in Fig. 12b, and (ii) a high crystalline structure for a typical GnP in Fig. 12c, demonstrating that it comprises possibly one graphene layer. This low thickness corresponds to the following low percolation threshold for electrical conductivity.

The electrical volume resistivity values of neat epoxy and its interface-modified nanocomposites were plotted against those of unmodified nanocomposites in Fig. 13, with detailed values shown in Table S1 and S2.† The resistivity was gradually reduced with the addition of m-GnPs, and eight orders of reduction was recorded at 0.489 vol%. 0.98 vol% m-GnPs produced a volume resistivity of $1.2 \times 10^8$ Ω cm. By contrast, no visible reduction was seen in the unmodified system. This is explained by the interface modification.

The modification causes two conflicting effects. On the one hand, the grafted organic molecules produce a barrier for the

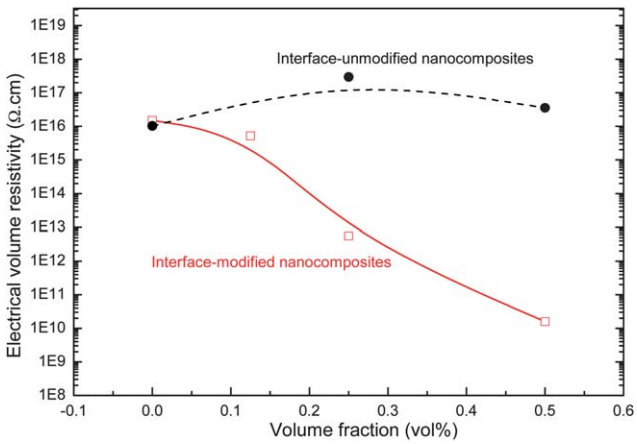


**Fig. 13** Electrical volume resistance of unmodified GnP and m-GnP nanocomposites.

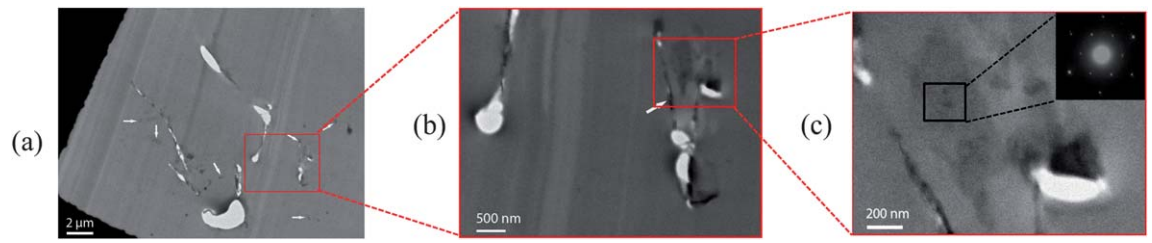


**Fig. 12** TEM micrographs of the 0.244 vol% epoxy/m-GnP nanocomposites.

GnPs-based conductive network, leading to a reduction in conductivity. The linking of adjacent layers during modification also means more fractions of GnPs needed to produce the network. On the other hand, the covalently bonded interface between the GnPs and matrix promotes the exfoliation and dispersion of GnPs, reducing the number and thickness of stacked GnPs, and this helps to form the network at a low GnP fraction. In the unmodified system, more GnPs stack themselves and are poorly dispersed, as indicated by the XRD analysis. It is well known that graphene exhibits poor through-plane conductivity, but its in-plane electrical conductivity is exceptionally high. Thinner GnPs undoubtedly have higher through-place conductivity. Thus, there are a larger number of separately dispersed, thinner m-GnPs in the modified system, and they can produce a conductive network at a lower fraction. Therefore, m-GnPs effectively reduce the electrical volume resistivity of epoxy.

Fracture toughness represents the resistance of a material to the propagation of a sufficiently sharp crack. Since obvious toughness improvements were reported in previous nanofiller-toughened epoxy resins,[25–32] we herein investigated the effect of interface on toughness and other mechanical properties.

Fig. 14 illustrates the fracture toughness $K_{1c}$ and critical strain energy release rate $G_{1c}$ of unmodified and modified GnP nanocomposites; Tables S3 and S4† contain detailed values. Both $K_{1c}$ and $G_{1c}$ increase steadily with the addition of GnPs, with the unmodified system displaying almost linear progression. With 0.489 vol% GnPs, $K_{1c}$ increases from 0.653 to 1.41 MPa $m^{1/2}$, a 115.9% improvement, and $G_{1c}$ from 176 to 521 J $m^{-2}$, 196.0%; the modified system demonstrates further improvements—65.9% for $K_{1c}$ and 84.6% for $G_{1c}$—in comparison with unmodified nanocomposites. These enhancements can be explained by the GnP filler absorbing fracture energy and preventing the propogation of cracks from developing further. The covalently bonded interface would (i) increase interface strength promoting a better degree of the GnP dispersion and exfoliation and impeding the debonding between GnPs and matrix which consumes more energy, and (ii) produce more thinner GnPs creating barriers to the crack propogation.

Young's moduli and tensile strength of neat epoxy and the unmodified and modified nanocomposites are illustrated in Fig. 15. It is noticeable that the modulus increases with GnP fractions, moreover, the increase is far more substantial in the modified GnP system with an increase of 57.4% at 0.489 vol%. The 47.7% higher modulus increments in the modified system must be caused by (i) a more homogenous dispersion of GnPs due to the modification; (ii) less platelets stacking leading to a larger interface area and a larger number of platelets in a unit volume, which share more stress under loading; (iii) the covalent bonding facilitating stress transfer from matrix to GnPs. These higher modulus improvements align with our previous

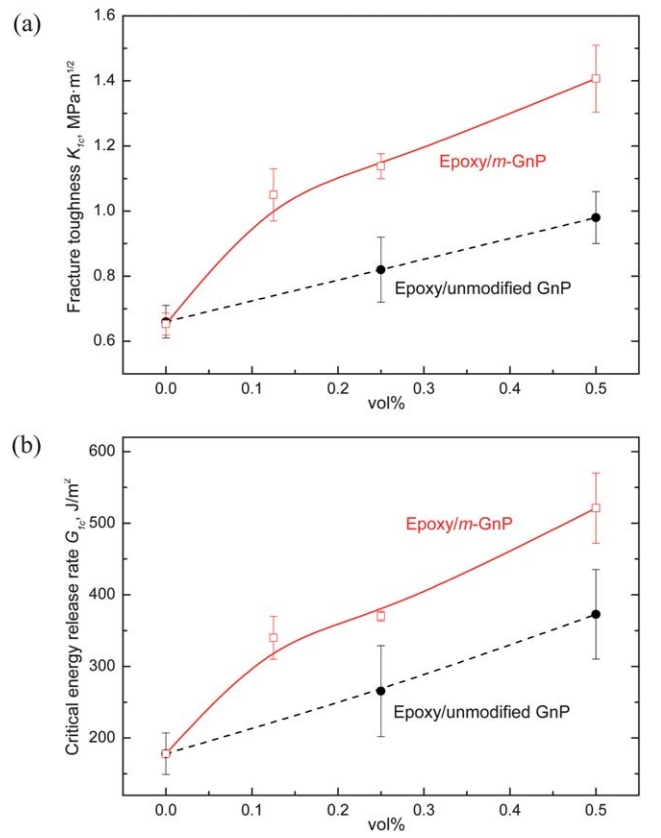


**Fig. 14** Fracture toughness and fracture energy release rate of neat epoxy and its unmodified GnP and m-GnP nanocomposites.

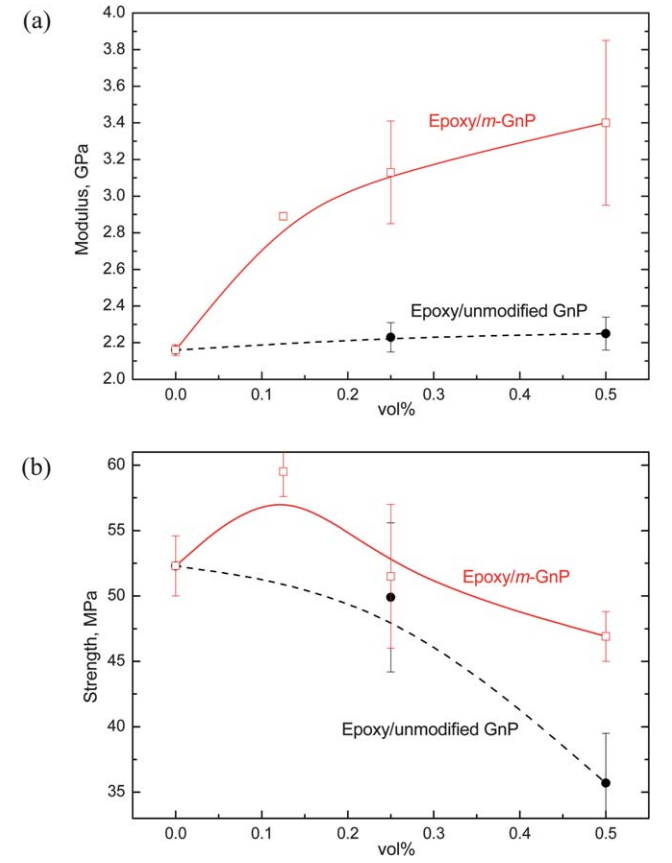


**Fig. 15** Young's modulus and tensile strength of neat epoxy and its unmodified GnP nanocomposites and m-GnP nanocomposites.

work on the interface modification of nanolayers-based composites.[16,25]

On account of the interface modification, the tensile strength peaks at 0.122 vol% and then slightly reduces. In comparison, the tensile strength obviously reduces in the unmodified system. At 0.489 vol% GnPs, the modified system shows a 10.3% reduction in tensile strength in comparison with 37.8% for the unmodified one. This remarkable difference in the stiffness and strength of these two systems is explained in light of the interface modification.

Defined as the distinct region between the dispersion phase and matrix, the interface is always a focal point in transferring stress and restraining the matrix molecular deformation upon loading. The overall characteristics of a composite are influenced by the nature of the interface with regard to mechanical strength, electron and phonon transmission, and resistance to chemical attack. The interface effect is more pronounced in nanocomposites due to the nanoparticles having a much larger surface area and significantly smaller distance than micron-sized particles. This enables nanocomposites to avoid the disadvantages of the severe loss of stiffness and/or strength by (i) reducing their filler volume fraction without sacrificing the reinforcing or toughening effect and (ii) having high levels of interaction between nanoparticles themselves and between nanoparticles and matrix at a low volume fraction.

Due to the high surface area to volume ratio ($\sim$0.67 $nm^{-1}$) of the layer-structured nanofiller, the interface plays a significant role, in comparison with spherical particles which have surface to volume ratios of generally lower than 0.2 $nm^{-1}$.[25–31] However, this high ratio of GnPs would diminish or disappear if GnPs stack in the matrix. Only interface modification prevents GnPs stacking, and this is confirmed by the foregoing XRD and conductivity analysis. The covalent interface modification also bridges GnPs with the matrix, allowing for more loading to be shared and for more matrix molecular deformation to be retained by GnPs.

Since silicate layers and carbon nanotubes have been extensively studied for polymer nanocomposites over the past two decades, we compared the mechanical properties and toughness of our interface-modified nanocomposites with those toughened by silicate layers and multi-walled carbon nanotubes in Table 2. At similar fractions, our nanocomposites show far high improvements in modulus and toughness. Given the low cost of GnPs (10–20 US$ per kg), our GnPs would be a promising filler for development of graphene-based devices and functional polymer nanocomposites.

## 4 Conclusions

Interface modification is found to play a crucial role in the structure and functional and mechanical properties of polymer/graphene nanocomposites. Current polymer/graphene studies lack effective methodologies for covalently bonded interface modification for resembling graphene's extraordinary properties as closely as possible. We adopted a cost-effective method to fabricate graphene platelets (GnPs) of 2.51 $\pm$ 0.39 nm in thickness. After our covalent modification, the m-GnP thickness increased to 6.4 $\pm$ 2.6 nm. Compared with unmodified nanocomposites, the interface-modified system shows eight orders of reduction in electrical resistivity at 0.489 vol% m-GnPs. $K_{1c}$ increases from 0.653 to 1.41 MPa $m^{1/2}$, a 115.9% improvement, and $G_{1c}$ from 176 to 521 J $m^{-2}$, 196.0%. Addition of nanolayers into a stiff polymer matrix often reduces tensile strength. At 0.489 vol%, the modified system shows a 10.3% reduction in tensile strength in comparison with 37.8% for the unmodified one. This study would provide a promising method for the interface modification of polymer/graphene nanocomposites for various applications.

## Acknowledgements

The authors thank B Wade and J Terlet for technical support at Adelaide Microscopy. JM thanks Asbury and Huntsman (Melbourne) for providing the graphite intercalation compound and Jeffamine D230, respectively. JM appreciates the early lab work conducted by Alex Sovi and Sanjay S. Chelliah.

## References

1 D. Li and R. B. Kaner, *Science*, 2008, **320**, 1170–1171.
2 S. Park and R. S. Ruoff, *Nat. Nanotechnol.*, 2009, **4**, 217–224.
3 T. Kuilla, S. Bahdra, D. Yao, N. H. Kim, S. Bose and J. H. Lee, *Prog. Polym. Sci.*, 2010, **35**, 1350–1375.
4 D. Li, M. B. Muller, S. Gilje, R. B. Kaner and G. G. Wallace, *Nat. Nanotechnol.*, 2008, **3**, 101–108.
5 I. Zaman, H. C. Kuang, Q. Meng, A. Michelmore, N. Kawashima, T. Pitt, L. Zhang, S. Gouda, L. Luong and J. Ma, *Adv. Funct. Mater.*, 2012, **22**, 2735–2743.
6 V. H. Pham, H. D. Pham, T. T. Dang, S. H. Hur and J. S. Chung, *J. Mater. Chem.*, 2012, **22**, 10530–10536.
7 I. Zamman, H. C. Kuan, J. Dai, N. Kawashima, A. Michelmore, L. Luong and J. Ma, *Nanoscale*, 2012, **4**, 4578–4586.

**Table 2** Comparison of ours with previous studies of nano-toughened epoxy

| Materials | Filler fraction (wt%) | Modulus increase (%) | $K_{1c}$ increase (%) | $G_{1c}$ increase (%) | Ref. |
|---|---|---|---|---|---|
| Epoxy/m-GnPs | 1.0 | 57.4 | 115.9 | 196.0 | Ours |
| Epoxy/clay | 2.5 | 16.7 | 58.5 | 114.9 | 33 |
| Epoxy/clay | 3.5–7.0 | 2.8 | 67.1 | 158.3 | 34 |
| Epoxy/MWCNT | 0.3–0.5 | 6.9 | 23.1 | N/A | 35 |
| Epoxy/MWCNT | 0.2–0.5 | 12.4 | 42.0 | 67.7 | 36 |

8 J. C. Meyer, A. K. Geim, M. I. Katsnelson, K. S. N. T. J. Booth and S. Roth, *Nature*, 2007, **446**, 60–63.
9 M. Fang, K. Wang, H. Lu, Y. Yang and S. Nutt, *J. Mater. Chem.*, 2009, **19**, 7098–7105.
10 Y. Zhu, S. Murali, W. Cai, X. Li, J. W. Suk, J. R. Potts and R. S. Ruoff, *Adv. Mater.*, 2010, **22**, 3906–3924.
11 R. Verdejo, M. M. Bernal, L. J. Romasanta and M. A. Lopez-Manchado, *J. Mater. Chem.*, 2011, **21**, 3301–3310.
12 M. Terrones, O. Martin, M. Gonzalez, J. Pozuelo, B. Serrano, J. C. Cabanelas, S. M. Vega-Diaz and J. Baselga, *Adv. Mater.*, 2011, **23**, 5302–5310.
13 X. Xia, Q. Hao, W. Lei, W. Wang and X. Wang, *J. Mater. Chem.*, 2012, **22**, 8314–8320.
14 J. Liu, J. Tang and J. J. Gooding, *J. Mater. Chem.*, 2012, **22**, 12435–12452.
15 H. Liu, J. Xu, Y. Li, B. Li and J. Ma, *Macromol. Rapid Commun.*, 2006, **27**, 1603.
16 I. Zaman, T. T. Phan, H. C. Kuan, Q. S. Meng, L. Luong and J. Ma, *Polymer*, 2011, **52**, 1603–1611.
17 J. Ma, Q. Qi, J. Bayley, X. Du and L. Zhang, *Polym. Test.*, 2007, **26**, 445.
18 Q. Meng, I. Zaman, I. Hannan and J. Ma, *Polym. Test.*, 2011, **30**, 243–250.
19 E. C. Mattson, H. Pu, S. Cui, M. A. Schofield, S. Rhim, G. Lu, *et al.*, *ACS Nano*, 2011, **5**, 9710–9717.
20 R. Larciprete, S. Fabris, T. Sun, P. Lacovig, A. Baraldi and S. L. Izzit, *J. Am. Chem. Soc.*, 2011, **133**, 17315–17321.
21 J. E. McMurry, *Organic Chemistry*, Thomson-Brooks/Cole, Belmont, CA, 6th edn, 2004, ch. 12, pp. 406–415.
22 E. Pretsch, P. Buhlmann and M. Badertscher, *Structure determination of organic compounds*, Springer, 4th edn, 2009, ch. 7, pp. 269–355.
23 U. Khan, H. Porwal, A. Neil, K. Nawaz, P. May and J. N. Coleman, *Langmuir*, 2011, **27**, 9077–9082.
24 A. Neil, U. Khan, P. May, J. Boland and J. N. Coleman, *J. Phys. Chem. C*, 2011, **115**, 5422–5428.
25 I. Zaman, Q. H. Le, H. C. Kuan, N. Kawashima, L. Luong and J. Ma, *Polymer*, 2011, **52**, 497–504.
26 Q. H. Le, H. C. Kuan, J. B. Dai, I. Zaman, L. Luong and J. Ma, *Polymer*, 2010, **51**, 4867–4879.
27 J. Ma, L. T. La, I. Zaman, L. Luong, D. Ogilvie and H. C. Kuan, *Macromol. Mater. Eng.*, 2011, **296**, 465–474.
28 S. C. Kuan, J. B. Dai, X. S. Du and J. Ma, *J. Appl. Polym. Sci.*, 2010, **115**, 3265–3272.
29 J. B. Dai, S. C. Kuan, S. C. Dai and J. Ma, *Polym. Int.*, 2009, **58**, 838–845.
30 J. Ma, M. Mo, X. S. Du, P. Rosso, K. Friedrich and H. C. Kuan, *Polymer*, 2008, **49**, 3510–3523.
31 J. Ma, M. Mo, X. S. Du, S. C. Dai and I. Luck, *J. Appl. Polym. Sci.*, 2008, **110**, 304–312.
32 S. Q. Li, F. Wang, Y. Wang, J. W. Wang, J. Ma and J. Xiao, *J. Mater. Sci.*, 2008, **43**, 2653–2658.
33 I. Zaman, Q. Le, H. C. Kuan, N. Kawashima, L. Luong, A. Gerson and J. Ma, *Polymer*, 2011, **52**, 497–504.
34 A. S. Zerda and A. J. Lesser, *J. Polym. Sci., Part B: Polym. Phys.*, 2001, **39**, 1137–1146.
35 F. H. Gojny, M. H. G. Wichmann, B. Fiedler and K. Schulte, *Compos. Sci. Technol.*, 2005, **65**, 2300–2313.
36 T. H. Hsieh, A. J. Kinloch, A. C. Taylor and I. A. Kinloch, *J. Mater. Sci.*, 2011, **46**, 7525–7535.

 